

Subwavelength silicon microcavities

Jeffrey Shainline¹, Stuart Elston¹, Zhijun Liu², Gustavo Fernandes², Rashid Zia² and Jimmy Xu^{1,2}

¹*Department of Physics, 184 Hope St., Brown University, Providence, RI 02912*

²*Division of Engineering, 184 Hope St., Brown University, Providence, RI 02912*

We present a study of the first subwavelength silicon microdisk resonators. To our knowledge, these are the smallest microcavities to be probed with tapered fiber spectroscopy or directly coupled to a waveguide. Spectral details of whispering gallery modes with azimuthal mode number $m = 4-7$ are measured in microdisks with diameters between $1.38-1.89\mu\text{m}$. For the structures considered here, $m = 5$ is the highest azimuthal mode number in a subwavelength cavity and has measured $Q = 1250$. These results agree well with theoretical calculations using the finite difference frequency domain method and fit an exponential scaling law relating Q to disk radius via m .

Planar lightwave circuits face the challenge of entering a market dominated by electronics whose progress has been driven by Moore's law and the ability to fabricate consistently smaller transistors. For photonic circuits, a physical size constraint emerges; the characteristic limiting size is the wavelength of light traversing the circuit. To overcome this physical limitation a great deal of research has recently been conducted to explore the potential of structures at and below this size limit to store and generate light. Beginning with the original demonstration of wavelength-scale microdisk lasers [1,2], more recent demonstrations have shown that structures smaller than the wavelength of light in all three spatial dimensions can give rise to laser action, but only at cryogenic temperatures [3-5]. However, a thorough experimental study of passive resonant cavities has not yet been conducted for cavities of characteristic dimension comparable to or smaller than the wavelength.

In this work we studied silicon microdisks of diameters ranging from smaller to larger than the wavelength corresponding to resonances of azimuthal mode number (m) from 2 to 7 with resonant wavelengths from $1.52\mu\text{m}$ to $1.62\mu\text{m}$. We have quantified the relationship between the radiation-limited quality factor (Q) and m using tapered fiber spectroscopy and compared our results to finite-difference frequency-domain (FDFD) simulations. The $m = 5$ mode was the mode of highest m in a subwavelength disk and was measured to have radiation-limited $Q = 1250$, indicative of a greater potential for laser operation than previously anticipated or achieved.

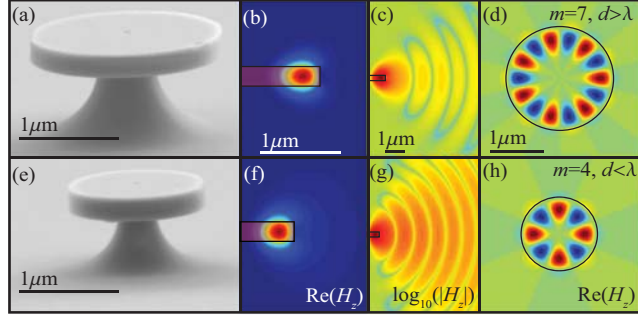


Fig. 1. Fabricated structures and calculated field profiles of microdisks for $m=7$ and $m=4$ modes. a) Disk of $1.89\mu\text{m}$ diameter. b) $\text{Re}(H_z)$ field profile of $m=7$ mode in the y - z plane calculated with the FDFD method. $Q \sim 20,000$. c) Far field ($\log_{10}(|\text{Re}(H_z)|)$) for the same disk. d) $\text{Re}(H_z)$ in the x - y plane calculated analytically. e) Disk of $1.35\mu\text{m}$ diameter. f-h) Calculations corresponding to those in b-d for the $1.35\mu\text{m}$ disk.

Resonances in microdisks can be classified according to three mode numbers corresponding to quantization in the vertical, radial and azimuthal directions [6]. To completely specify the mode one must also specify the polarization as TE-like (H_z is the dominant field component) or TM-like (E_z is the dominant field component). The highest- Q resonances occur when the wave vector is predominantly in the azimuthal direction [7]. Therefore, we consider only modes of fundamental order in the vertical and radial direction and classify modes by m . Further, the partial differential equation describing the system is separable, and the equation governing the z -dependence is identical to that of a slab waveguide. This equation can be solved to obtain an effective index of refraction, which is larger for the case of TE modes than for TM [6]. For this reason we consider only TE modes in this study.

In order to make quantitative predictions about the microdisk modal characteristics, we have used both analytical and numerical methods. Specifically, we investigated the analytical dispersion relations for microdisk whispering gallery modes by solving the appropriate boundary value problem [6-8], and we calculated the quasinormal modes of microdisk resonators using an FDFD mode solver. Adapting the approach described in refs. (9) and (10), these FDFD calculations leveraged the azimuthal symmetry of the modes (i.e. the $\exp(im\phi)$ dependence) to semi-analytically reduce the 3D resonator geometry to a transverse 2D eigenvalue problem. This full-vectorial method allowed for calculations of all electromagnetic field components as well as the effective mode volume [11], Purcell enhancement [12] and bending-limited finesse [7].

Several techniques for fabricating microdisks result in angled sidewalls [11,13,14]. In some cases the angled sidewalls arise from fabrication steps which produce smoother sidewalls. Smooth sidewalls are of critical importance for microdisks which are not operating in the radiation-limited- Q regime, as Rayleigh scattering from sidewall imperfections are usually the dominant loss mechanism in such disks [13]. However, our theoretical and experimental experience informs us that in the subwavelength regime sidewall verticality is a greater concern

than minor sidewall roughness. Silicon microdisks were fabricated on SOI (250nm silicon layer, atop $3\mu\text{m}$ oxide). To make disks with sidewalls which are vertical and yet as smooth as possible we perform negative electron beam lithography with PMMA [15] at a dosage of $2 \times 10^4 \mu\text{C}/\text{cm}^2$. At dosages of this magnitude, the polymer units of PMMA crosslink to form a material which is resistant to etchants. In our experiments, this technique has given rise to smoother sidewalls than simply performing positive lithography without resist reflow. The electron exposure is followed by development in acetone and ICP RIE with SF_6 and C_4F_8 . Photolithography and deep ICP RIE are then performed to etch through the $3\mu\text{m}$ SiO_2 insulator layer and through $\sim 30\mu\text{m}$ of the underlying silicon substrate. This isolates the disks on a strip which is lifted above the rest of the substrate and thus makes it easier access the disks with the tapered fiber. An undercut is performed with buffered hydrofluoric acid.

SEM images of two completed disks are shown in Fig. 1 along with the calculated near- and far-field profiles of their resonant modes. Contrasting Fig. 1 (b) and Fig. 1 (f) one sees the near-field amplitude extending further radially and axially in the subwavelength disk. Contrasting Fig. 1 (c) and Fig. 1 (g) one observes the increased far-field radiation emanating from the subwavelength cavity.

To experimentally characterize the disks we utilize the technique of tapered fiber spectroscopy [11,13,14,16]. A tunable laser sweeps the wavelength range from $1.52\mu\text{m}$ to $1.62\mu\text{m}$. The transmission through a tapered fiber coupled to a disk is monitored with an optical spectrum analyzer. The transmission dips are fit to a Lorentzian function and the Q factor is extracted from the width and center wavelength.

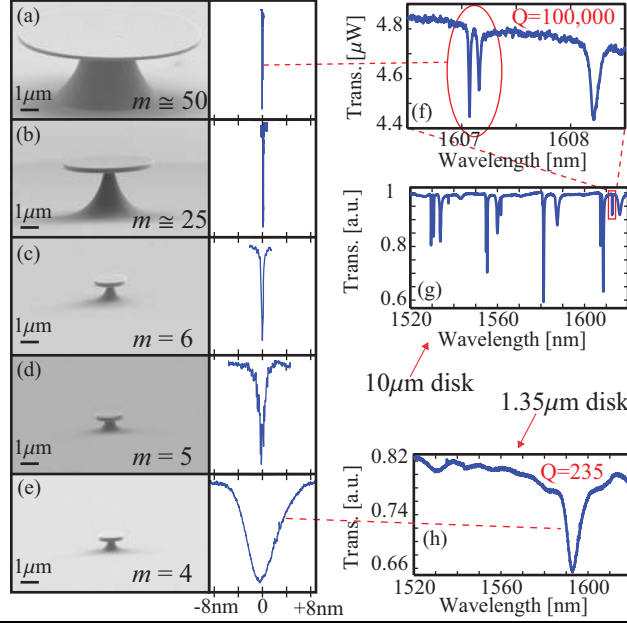


Fig. 2. Silicon microdisks of decreasing diameters and tapered fiber spectra. a-e) SEM images at of disks of diameter 10 μ m, 5 μ m, 1.70 μ m, 1.48 μ m and 1.35 μ m respectively. Resonant transmission dips in tapered fiber spectra acquired from the disks are shown. The y-axes of these plots are transmission in arbitrary units and the x-axis is wavelength detuning. f) High resolution tapered fiber spectrum of a 10 μ m disk. g) Scan of the full tunable laser range for the 10 μ m disk. h) Scan of the full tunable laser range for the m=4 mode.

Figure 2 shows SEM images of microdisks with diameters varying from 10 μ m—with radiation-limited Q on the order of 10^{13} (the Rayleigh-scattering-limited Q in this disk is $\sim 10^5$)—down to a subwavelength disk of approximately 1 μ m diameter with radiation-limited $Q = 235$. Next to each disc is a tapered fiber spectrum of the characteristic resonance of the disk. The SEM images depict the decrease in size over an order of magnitude while broadening of the resonances demonstrate the exponential decrease in Q factor. In Figs. 2(f)-(h) tapered fiber spectra of large and small disks are contrasted in more detail. Figure 2(f) shows a high-resolution scan of a 2nm wavelength window of a tapered fiber spectrum from a 10 μ m-diameter silicon disk. The doublet character of the high- Q mode is apparent. Figure 2(g) shows a scan of the entire tunable laser range for the same disk. The free spectral range is ~ 27 nm. The depth of a dip is an indication of the degree of coupling between the fiber and the disk. Stronger coupling to lower- Q , higher-radial-order modes is evident [14]. In Fig. 2(h) a tapered fiber spectrum of a 1.35 μ m disk is shown. The free spectral range is ~ 200 nm, and only one resonance is present. If one wishes to use whispering-gallery-mode microcavities for devices such as filters and switches, the large free spectral range of wavelength-scale microdisks is an attractive feature. Another attribute is that higher-radial-order modes do not exist in this wavelength range for a disk of this size. The other features of the spectrum in Fig. 2(h) are due to coupling to the substrate. Because these small

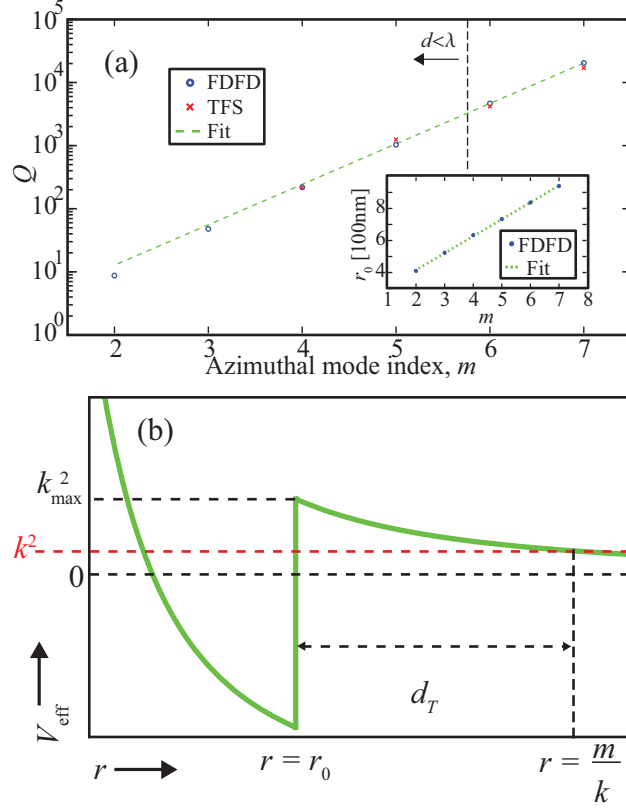


Fig. 3. Microdisk Q versus m . a) Experimental data, theoretical value obtained with FDFD and a fit to an exponential function are shown. The linear relationship between the disk radius, r_0 , and m is shown in the inset. b) The effective potential and tunneling parameters.

disks are only a few hundred nanometers from the substrate, coupling of the fiber to the substrate is more prominent than in larger disks.

In Fig. 3 we present a comparison of the experimentally-obtained Q factors with the theoretical radiation-limited Q factors obtained with FDFD calculations. The theoretical curve is obtained by varying the disk radius, r_0 , to obtain a resonance for each integer $m = 2-7$ within a few nanometers of $1.57\mu\text{m}$, the center of our tunable laser range. The experimental points are acquired using tapered fiber spectroscopy as described above. Each experimental data point is from a disk of a different radius. The excellent agreement between experiment and theory indicates that our silicon microdisks have radiation-limited Q factors that are not significantly degraded by minor sidewall perturbations. It should be noted that the measured resonance at $m = 7$ was a doublet mode, as discussed in refs. (11,13,16,17). The splitting was only observed for the $m = 7$ mode where the Lorentzian is narrow enough to differentiate the two peaks. We find that the $m = 5$ mode is the subwavelength mode of highest m with measured $Q = 1250$. The diameter of the disk was $1.49\mu\text{m}$ and resonant wavelength was $1.543\mu\text{m}$ giving a ratio of $d/\lambda = 0.967$. The $m = 4$ mode was observed in a cavity of diameter $1.35\mu\text{m}$ at wavelength of $\lambda = 1.591\mu\text{m}$ giving $d/\lambda = 0.849$. Due to the limited wavelength window accessible by our tunable laser, and the broad nature of the low- Q $m = 3$ mode, it was not observed in our studies. The theoretical value

of $d/\lambda = 0.683$. Below $m = 3$ the resonances have $Q < 10$. To create microdisks with well defined resonances for $m < 3$ and $d/\lambda < 0.7$, metallodielectric architectures, which trade ohmic loss for suppressed radiation, may offer advantages [5,14].

Analysis of our data reveals that m has a linear relationship with r_0 over the range $m = 2-7$ at a (nearly) constant wavelength. Q has an exponential dependence on m of the form $Q(m) = A \exp(\chi m)$, where $A = 0.666$ and $\chi = 1.48$ are parameters which have been determined with non-linear regression. As seen in Fig. 3, this expression fits our data quite well over the range of m values considered here. The linear dependence of m on r_0 can be understood because the mode propagates around the circumference of the disk. The effective mode volume also has a linear dependence on m . Thus, the Purcell enhancement decays exponentially with decreased m , as does the finesse [7].

The exponential dependence of Q on m can be understood in the framework of the effective potential, which is given by $V_{\text{eff}}(r) = k^2 [1 - n_{\text{eff}}^2(r)] + m^2/r^2$ [18] and is plotted in Fig. 3(b). This quantity enters the scalar radial equation for the dominant field component if TE or TM polarization is assumed. In this expression, $n_{\text{eff}}(r)$ is the effective index of refraction of the disk. It is a function of r in that it changes discontinuously from its value inside the disk (~ 2.8 for the parameters considered here) to unity beyond r_0 . Thus, V_{eff} changes discontinuously at the edge of the disk, creating a potential well in which the electromagnetic field predominantly resides. There are two features of a potential which affect the tunneling probability—the barrier height and barrier width. For a given wavelength, the height of the tunneling barrier scales as m^2/r_0^2 . In a general one-dimensional tunneling scenario, the tunneling probability will have a power law dependence on barrier height. Therefore, the quadratic dependence of the barrier height on m cannot explain the exponential dependence of Q on m . However, the tunneling probability through a one-dimensional barrier is exponentially dependent on the barrier width. As shown in Fig. 3, the radial distance at which the confined mode can emerge to free space is $r = m/k$, and is determined by the condition $V_{\text{eff}} = k^2$. Thus, the tunneling barrier thickness is given by $d_T = m/k - r_0$. Using the linear relationship between m and r_0 ($r_0 = sm + b$) the tunneling thickness is $d_T = (1/k - s)m - b$. Thus, $1/Q(m) \propto T(m) \propto \exp[-\kappa d_T(m)] \propto \exp[-\kappa' m]$, where T is the tunneling probability and κ and κ' are unknown constants which could be determined from a rigorous treatment. Thus, the exponential dependence of Q on m (and r_0) is consistent with the linear dependence of tunneling barrier width on m .

In conclusion, we have investigated the resonant modes of silicon microdisks that are smaller in every dimension than the free-space wavelength of light being stored in the cavity. We have presented a systematic characterization of the $m = 2-7$ modes and have quantified the linear relationship between m and r_0 as well as the exponential dependence of Q on m . Our experimental data is in excellent agreement with theoretical values for the radiation-limited Q . We have demonstrated the $m = 5$ mode is the highest- Q mode in a subwavelength disk and was

measured in our structures to have a $Q = 1250$ at a wavelength of $1.543\mu\text{m}$ in a microdisk of diameter $1.490\mu\text{m}$.

Acknowledgements: We are grateful to Dr. Gernot Pomrenke and the grant support of AFOSR (FA9550-07-1-0286).

- [1] S.L. McCall, A.F.J. Levi, R.E. Slusher, S.J. Pearton and R.A. Logan, "Whispering-gallery mode microdisk lasers," *Appl. Phys. Lett.* **60**, 289-291 (1992).
- [2] A.F.J. Levi, S.L. McCall, S.J. Pearton and R.A. Logan, "Room temperature operation of submicrometre radius disk laser," *Elect. Lett.* **29**, 1666-1667 (1993).
- [3] M. T. Hill, Y.-S. Oei, B. Smalbrugge, Y. Zhu, T. De Vries, P.J. Van Veldhoven, F.W.M. Van Otten, T. J. Eijkemans, J.P. Turkiewicz, H. De Waardt, E.J. Geluk, S.-H. Kwon, Y.-H. Lee, R. Notzel and M.K. Smit, "Lasing in metallic-coated nanocavities," *Nature Photonics* **1**, 589-593 (2007).
- [4] Q. Song, H. Cao, S.T. Ho and G.S. Solomon, "Near-IR subwavelength microdisk lasers," *Appl. Phys. Lett.* **94**, 061109-1-061109-3 (2009).
- [5] C. Manolatou and F. Rana, "Subwavelength nanopatch cavities for semiconductor plasmon lasers," *IEEE J. Quant. Elec.* **44**, 435-447 (2008).
- [6] K. Zhang and D. Li, *Electromagnetic Theory for Microwaves and Optoelectronics* (Springer, 1998).
- [7] J.E. Heebner, T.C. Bond and J.C. Kallman, "Generalized formulation for performance degradations due to bending and edge scattering loss in microdisk resonators," *Opt. Expr.* **15**, 4452-4473 (2007).
- [8] R.P. Wang and M.-M. Dumitrescu, "Optical modes in semiconductor microdisk lasers," *IEEE J. Quant. Elec.* **34**, 1933-1937 (1998).
- [9] P. Lusse, P. Stuwe, J. Schule and H.-G. Unger, "Analysis of vectorial mode fields in optical waveguides by a new finite difference method," *J. Lightwave Technol.* **12**, 487-494 (1994).
- [10] R. Zia, M.D. Selker, and M.L. Brongersma, "Leaky and bound modes of surface plasmon waveguides," *Phys. Rev. B* **71**, 165431 (2005).
- [11] K. Srinivasan, M. Borselli, O. Painter, A. Stintz and S. Krishna, "Cavity Q, mode volume, and lasing threshold in small diameter AlGaAs microdisks with embedded quantum dots," *Opt. Expr.* **14**, 1094-1105 (2006).

- [12] H. Benisty, J.-M. Gerard, R. Houdre, J. Rarity and C. Weisbuch, Eds. *Confined Photon Systems* (Springer, 1998).
- [13] M. Borselli, T.J. Johnson and O. Painter, “Beyond the Rayleigh scattering limit in high- Q silicon microdisks: theory and experiment,” *Opt. Expr.* **13**, 1515-1530 (2005).
- [14] B. Min, E. Ostby, V. Sorger, E. Ulin-Avila, L. Yang, X. Zhang and K. Vahala, “High- Q surface-plasmon-polariton whispering-gallery microcavity,” *Nature* **457**, 455-458 (2009).
- [15] A.C.F. Hoole, M.E. Welland and A.N. Broers, “Negative PMMA as a high-resolution resist—the limits and possibilities,” *Semicond. Sci. Technol.* **12**, 1166-1170 (1997).
- [16] M. Borselli, K. Srinivasan, P.E. Barclay and O. Painter, “Rayleigh scattering, mode coupling and optical loss in silicon microdisks,” *Appl. Phys. Lett.* **85**, 3693-3695 (2004).
- [17] L. Deych and J. Rubin, “Rayleigh scattering of whispering gallery modes of microspheres due to a single scatterer: myths and reality.” arXiv:0812.4404v1 [physics.optics] 23 Dec 2008
- [18] Jens Uwe Nöckel, “Resonances in nonintegrable open systems,” Ph.D. thesis, Yale University, 1997.